Journal of Hydrology 520 (2015) 123–133

Contents lists available at ScienceDirect

Journal of Hydrology

journal homepage: www.elsevier.com/locate/jhydrol

Water flow and nitrate transport through a lakeshore with different revetment materials

Yong Li [a,b,*], Jirka Šimůnek [c,*], Zhentin Zhang [b], Manli Huang [b], Lixiao Ni [b], Liang Zhu [b], Jianlan Hua [d], Yong Chen [d]

[a] Ministry of Education Key Laboratory of Integrated Regulation and Resource Development on Shallow Lakes, Hohai University, Nanjing 210098, China
[b] College of Environment, Hohai University, Nanjing 210098, China
[c] Department of Environmental Sciences, University of California Riverside, Riverside, CA 92521, USA
[d] Nanjing Water Planning and Designing Institute Co. Ltd, Nanjing 210006, China

ARTICLE INFO

Article history:
Received 6 June 2014
Received in revised form 10 November 2014
Accepted 15 November 2014
Available online 22 November 2014
This manuscript was handled by Corrado Corradini, Editor-in-Chief, with the assistance of Stephen Worthington, Associate Editor

Keywords:
Lakeshore
Groundwater
Flow regime
Nitrate
Slope revetment material
Hydrus-2D

SUMMARY

As an important part of a transition zone surrounding a lake, lakeshore plays a critical role in connecting hydrology and biochemistry between surface water and groundwater. The shape, slope, subsurface features, and seepage face of a lakeside slope have been reported to affect water and nutrient exchange and consequently the water quality of near-shore lake water. Soil tank experiments and Hydrus-2D model simulations were conducted to improve our understanding of the influence of slope revetment materials (SRMs) on water flow and solute transport in a lakeshore zone. The low hydraulic conductivity of SRMs affected flow patterns in the lakeshore zone and resulted in a local increase of the groundwater table near the slope face. Water and solute flux distributions on the slope face under bare-slope conditions followed an exponential function. Fluxes were concentrated within a narrow portion of the slope surface near the intersection point between the lake water level and the slope face. Surface pollutants (for example from fishponds and paddy fields surrounding a lake) were transported into the lake along shallow groundwater through both unsaturated and saturated zones. The SRMs on the slope face affected the ratio of water and solute fluxes in the unsaturated zone, increasing along with the decline of the hydraulic conductivity of SRMs. Furthermore, as the hydraulic conductivity of SRMs decreased, the retention time and the potential for oxygen reduction correspondingly increased, which affected the nitrogen transport and transformations in the lakeshore zone. Simulated and experimental results indicate that if concrete along the shoreline of Lake Taihu is replaced with a relatively high-conductivity lime or the slope is left bare, water fluxes will increase less than solute fluxes, which will rise significantly, in particular in the unsaturated zone and along the seepage face. On the other hand, the largest water and solute fluxes along the shoreline for the bare and lime-slope conditions will be located higher at the slope than for the concrete-slope conditions. Hydrus-2D provided a good description of complicated hydrodynamic and solute transport/transformation conditions in the lakeshore zone.

1. Introduction

Lakeshore is an important component of the transitional zone surrounding a lake and plays a critical role in connecting hydrological and biogeochemical cycles of near- and off-shore regions (Ostendorp, 2004). Lake water, groundwater, and soil water mutually interact in the lakeshore zone, while pollutants are subject to concurrent transport and transformation processes under these complex hydrological conditions. The lakeshore zone is often considered an effective buffer region that retards pollution from surrounding land areas before it enters into lake water (Howarth et al., 2011). Recently, increasing attention has been given to the importance of a riparian zone (including a lakeshore) and attenuation of nitrates and other pollutants in this region (Ostendorp, 2004; Burgin and Groffman, 2012). A large number of studies have been carried out evaluating the effects of the slope, width, and shape of a lakeshore on hydrological and solute cycles in this zone (Cey et al., 1998; Genereux and Bandopadhyay, 2001; Li et al., 2007; Zhu et al., 2012). However, the effects of different slope revetment materials (SRMs) used on a lakeshore slope on hydrological and biogeochemical processes still have not been thoroughly studied.

* Corresponding authors at: Ministry of Education Key Laboratory of Integrated Regulation and Resource Development on Shallow Lakes, Hohai University, Nanjing 210098, China (Y. Li).
E-mail addresses: liyonghh@hhu.edu.cn (Y. Li), Jiri.Simunek@ucr.edu (J. Šimůnek).

http://dx.doi.org/10.1016/j.jhydrol.2014.11.045
0022-1694/

In essence, SRMs used on the waterside slope affect local hydraulic conductivities (Mohamed, 2006) and consequently the flow direction and fluxes, flow pathways, retention times, and even the soil reduction–oxidation potential (Lee, 2000; Lassabatere et al., 2004; Bouazza et al., 2006). The hydraulic conductivity of the near shore region significantly affects inflow/outflow hydrodynamics of a shoreline (Lee, 2000). Genereux and Bandopadhyay (2001) reported for inflow lakes that adding low-conductivity lake sediments, and decreasing their conductivity, produced a shift of groundwater seepage further offshore. Increasing the anisotropy of the surrounding porous medium had the same effect.

SRMs used in China mainly include concrete (with an extremely low conductivity), but also other materials such as ecological concrete (with a medium–high conductivity), lime with geotextiles (with a relatively low conductivity), and other materials (Wang and Luo, 2006; Yao and Yue, 2012). The present shoreline of Lake Taihu, the third largest freshwater lake in China, is almost entirely covered by a concrete material on the waterside slope in order to protect people and agricultural crops against floods (Hu et al., 2011). During the past several decades, the importance of the concrete lake shoreline to prevent erosion due to floods and wind waves could not been questioned. Nevertheless, as public preference for natural landscaping increased in importance and the near-shore lake water quality decreased, detrimental functions of the concrete lakeshore started to be discussed and questioned. Some researchers have suggested that the concrete shoreline should be replaced with materials that are more natural in order to rebuild the connection between near-shore and off-shore zones. Some have suggested that the lake shoreline should be returned to natural conditions (namely natural soils with grass) (Yang et al., 2005; Shaw et al., 2011). Others have insisted that the flood control function of the lake shoreline should be preserved by using a low conductivity material with embedded geotextiles (Nahlawi et al., 2007; Lamy et al., 2013). However, it is not well understood how such changes would alter hydrological and biogeochemical processes in the lakeshore zone. Hydraulic coupling between Lake Taihu and groundwater is difficult to assess through in-situ observations because of the presence of the concrete material at the lake shoreline. Therefore, before making any engineering decisions, preliminary studies have to be carried out to evaluate the effects of different SRMs on hydrological and biochemical processes in the lakeshore zone. More research is also definitely needed to evaluate the effects of the lake water level on shoreline groundwater processes (Schneider et al., 2005).

The exchange of water and solutes between groundwater and lakes is a complex process, and it is still a challenge to understand its temporal and spatial variability (Kidmose et al., 2011). Models are useful tools for identifying various hydrological factors that affect groundwater and solute discharge fluxes into sensitive surface water bodies such as lakes and wetlands (Lee, 2000; Simpson et al., 2003). The Hydrus-2D model, which has been used widely in similar research studies (e.g., Lee, 2000), was therefore used to simulate these processes in order to improve our understanding of water flow and nitrate transport processes in the lakeshore zone.

To improve our understanding of environments of lakeshore zones, we have conducted both laboratory soil tank experiments and corresponding numerical simulations using the Hydrus-2D model. Obtained data were analyzed to reveal general characteristics of water and nitrogen regimes in the lakeshore zone covered using three different SRMs. The effects of SRMs on distributions of water and solute fluxes on the slope face were studied in particular. Furthermore, relative fractions of water and solute fluxes passing through seepage face and submerged zones on the slope face were compared for the three SRM-cover conditions in order to better understand the transport pathways from land surface pollutant sources (for example from fish ponds or paddy fields).

2. Material and methods

2.1. Soil tank experiment

2.1.1. Design and set-up

A large soil tank (Fig. 1a) was used to simulate water flow and solute transport in the lakeshore zone. The tank was filled with soil layer by layer; each evenly compacted using a heavy object. The lakeside slope (α) was set at about 35°. Two thin PVC (Polyvinyl chloride) panels vertically divided the tank into three sections with different surface covers (Fig. 1b). Namely, one section was covered with a concrete material (with a low hydraulic conductivity), another section with a lime material (with a moderate conductivity), and the center section remained bare (additional soil was added to have the same embankment thickness). The SRMs (lime or concrete) only covered the upper section of the slope, while the lower section of the slope (beneath 30 cm) was filled with rocks. The groundwater table (GWT) was constant upstream (the HP boundary in Fig. 1a), supplied by two submerged pumps with flow meters. The lake water level (LWL, the AO boundary in Fig. 1a) was kept constant as well, controlled using overflow troughs with flow meters. The fishpond was set up on the land surface 95 cm away from the upstream boundary and its leaching flux (10 cm day^{-1}) with pollutants was controlled by one micro pump. Before the experiments, steady-state water flow conditions in the soil tank were established by maintaining constant water levels upstream (GWT) and downstream (LWL) for about one month. Selected soil physical and chemical properties are listed in Table 1.

Multiple experiments were concurrently carried out in three sub soil tanks, in order to better understand the effects of different SRMs on flow patterns and solute transport in the lakeshore zone. Based on field observations carried out in the lakeshore zone of Lake Taihu, average groundwater gradients were set at three typical values of 0.063, 0.043, and 0.022 m m^{-1}, corresponding to the dry (a LWL was 30 cm), normal (40 cm), and wet (50 cm) seasons, respectively (Fig. 1c). The GWT at the upstream boundary (line HP in Fig. 1a) was kept constant (60 cm) in all experiments. The ratio d/D represents the ratio between the relative distance from point O to the entire length of the slope face (D). Variables d_{30}, d_{40}, and d_{50} represent the distances on the slope face from point O to the intersection points B, C, and D of LWLs with the slope face, respectively (Fig. 1c).

Solutes were mixed into the assumed fishpond (or a paddy field) after a steady state water flow was reached. A solution of $NaNO_3$ and NaCl was mixed into the fishpond along with pumped water. The concentrations of chloride and nitrate were 10.0 mg L^{-1}. The experiment representing dry-season conditions was conducted first. After the experiment was finished, the soil tank was slowly flushed for about one month until solute concentrations at all observation points stabilized. Then, the experiment representing the normal season was carried out, followed by the experiment representing the wet season.

2.1.2. Measurements and analysis

Inflow fluxes through the upstream boundary (the HP line in Fig. 1a) were recorded using flowmeters connected with pumps. Groundwater table data were observed from scales connecting stainless steel tubes in the soil tank. The tubes were installed beneath the groundwater table 100, 200, 290, 420 and 465 cm away from the upstream boundary (Fig. 1a). Soil solutions were collected every ten days using porous ceramic suction cups at S_1–S_{11} (Fig. 1a). The residual solution in the suction cups was cleansed using an injector each time before sampling. The cups were then evacuated to about 80 kPa by a vacuum pump with a

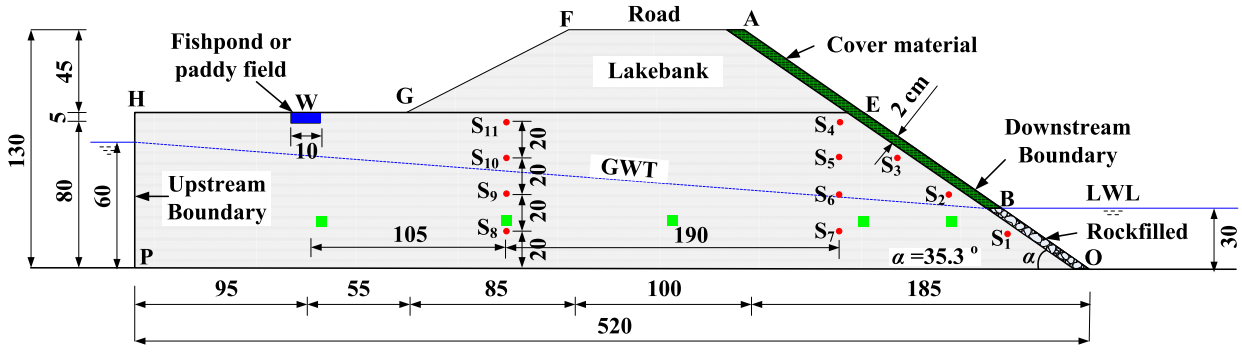

(a) Side view of the soil tank (solute concentration observation points (●:S_1-S_{11}) and groundwater table (GWT) observation points (■). LWL represents the lake water level).

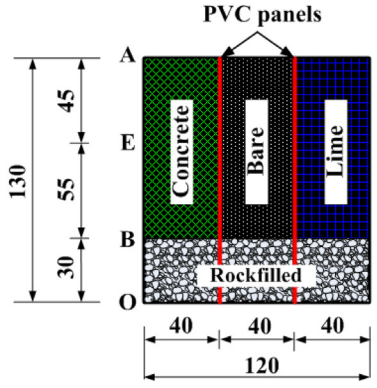

(b) Front view of the soil tank (PVC: polyvinyl chloride).

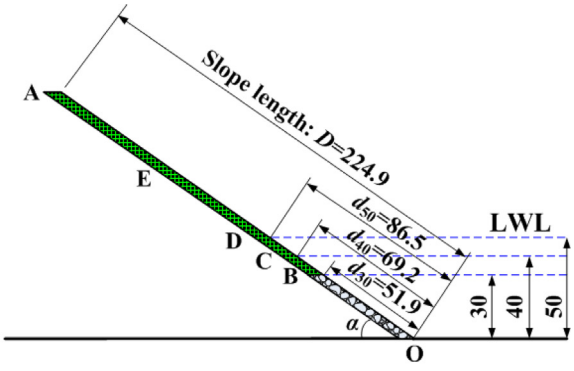

(c) Side view of the slope face.

Fig. 1. Schematic of the experimental set-up (a), slope revetment materials (b), and the detail of the slope face (c). All units are in cm.

Table 1
Physical and chemical properties of soil materials used in the soil tank experiments.

Layer	Soil particle size distribution (%)			Bulk density (g cm^{-3})	Organic matter (%)	pH (H_2O)
	Sand (>0.05 mm)	Silt (0.002–0.05 mm)	Clay (<0.002 mm)			
Lakeshore	87.4	10.2	2.4	1.43	0.18	6.9
Lime	58.9	31.4	9.7	1.59	0.10	7.4

tensiometer. The concentrations of chloride and nitrate were analyzed using a continuous flow auto-analyzer.

2.2. Hydrus-2D model

2.2.1. Model description

The Hydrus-2D model (Šimůnek et al., 2008) was concurrently used to simulate the laboratory tank experiments to improve our understanding of the flow and transport patterns in the lakeshore zone. Considering the two-dimensional isothermal uniform Darcian water flow in a variably-saturated rigid porous medium, and assuming that the air phase plays an insignificant role in the liquid flow process, the governing water flow and solute transport equations are given by the Richards and convection–dispersion equations, respectively. Both governing equations are numerically solved in Hydrus-2D using the method of finite elements. An appropriate spatial discretization is crucial to avoid numerical oscillations and to achieve acceptable mass balance errors (Šimůnek et al., 2008). The total number of triangular finite elements (FE) was 18,167 in all simulations. At the slope surface and near the fishpond (areas with large pressure head gradients), the size of FE was approximately 1 cm, while in other parts of the transport domain it was approximately 1–6 cm. Time steps were automatically controlled by the Hydrus-2D model within the initially specified range of 10^{-7} and 0.1 day. As suggested in the manual of the Hydrus-2D model for minimizing or eliminating numerical oscillations, the Peclet (*Pe*) and Courant (*Cr*) numbers were controlled by a stability condition "$Pe \times Cr \leqslant 2$" (Šimůnek et al., 2012).

2.2.2. Input parameters

The Hydrus-2D input parameters are required to characterize two main sets of processes: the soil hydraulic parameters for water flow and solute transport and reaction parameters for solute transport. The initial estimates of the van Genuchten (1980) soil

hydraulic parameters (θ_r, θ_S, α, and n: residual and saturated water contents, and two shape parameters, respectively) were estimated using the RETC software by fitting retention data, $\theta(h)$, measured using the pressure chamber apparatus. The pore connectivity parameter (l) was assumed equal to an average value (0.5) for many soils. The solute transport parameters were considered using the following values: the molecular diffusion coefficient in free water (D^w) for NO_3^- was 1.64 $cm^2\ day^{-1}$, the initial longitudinal dispersivity (α_L = 45 cm) was assumed to be one-tenth of the travel distance, and the initial transverse dispersivity (α_T = 4.5 cm) was considered to be equal to one-tenth of the longitudinal dispersivity (Gelhar et al., 1985; Phogat et al., 2012). Denitrification rates were initially assumed to be the same (namely K_{dn} = 0.02 day^{-1}) in all soil materials and then adjusted to 0.015 day^{-1} according to measured data.

2.2.3. Initial and boundary conditions

The initial distribution of the pressure head was set to decrease linearly with a unit gradient (hydrostatic equilibrium) from the bottom to the top of the soil profile. The initial chloride and nitrate contents in the soil were zero. The groundwater table at the upstream boundary was assumed to be 60 cm above the bottom of the soil profile. The groundwater table at the downstream boundary reflected the water level in the lake (LWL). A potential seepage face boundary condition was assigned to the part of the boundary above the LWL when there was no cover or when lime was placed on the slope. The nodes with an active seepage face were assigned a pressure head equal to zero. This part of the boundary was assigned a "no flow" boundary condition when concrete was present on the slope. A constant flux boundary condition (10 cm day^{-1}) was assigned to the boundary representing the fishpond. Evaporation was neglected in order to investigate only the effects of SRMs. A third-type boundary condition (a Cauchy boundary condition) was used at both upstream and downstream boundaries for solute transport.

2.3. Model evaluation

Simulated values of the groundwater table, total water fluxes, and chloride and NO_3^-–N concentrations in the soil were compared with the corresponding measured data from the soil tank experiments. The correspondence between simulated and observed data was evaluated using the coefficient of determination (r^2) at p = 0.05 and the root mean square error (*RMSE*). The *RMSE* was calculated as

$$RMSE = \sqrt{\frac{1}{n}\sum_1^n (S_i - M_i)^2}$$

where S_i and M_i are simulated and measured values, respectively, and n is the number of compared values. Optimum values of r^2 and *RMSE* are 1 and 0, respectively.

3. Results

3.1. Model calibration and validation

Observed GWTs and inflow fluxes were used to further calibrate the soil hydraulic parameters, obtained earlier from laboratory retention data, using Hydrus-2D. Simulated GWTs showed a good agreement with observed data (Fig. 2, *RMSE* = 0.39 cm, n = 54, r^2 = 0.97) for calibrated soil hydraulic parameters. Simulated groundwater fluxes into the lake were compared with total water fluxes, which included upstream inflow and fishpond leakage (*RMSE* = 26.4 $cm^2\ day^{-1}$, n = 108, r^2 = 0.96).

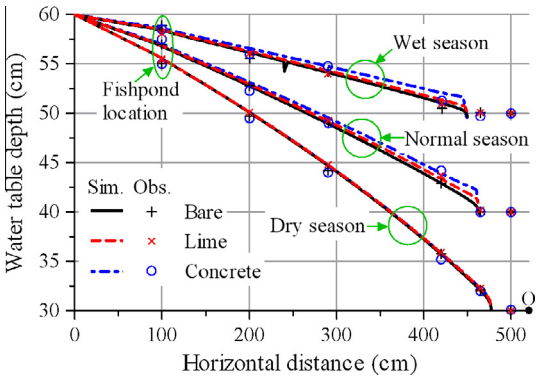

Fig. 2. Simulated and observed groundwater tables under bare-, lime-, and concrete-slope conditions during the dry, normal, and wet seasons. The letter "O" indicates the end of the slope (see also Fig. 1c). The water level at the upstream boundary was kept at 60 cm, while at the downstream boundary at 30 cm, 40 cm, and 50 cm to represent the dry, normal, and wet seasons. The horizontal distance is measured from the upstream boundary (as seen in Fig. 1a).

Chloride and nitrate concentrations observed in soil tank experiments with a bare slope face during the wet season were used to calibrate the transport and reaction parameters in Hydrus-2D. Selected calibration results for chloride and nitrate concentrations at six observation points near the lakeshore zone, namely S_1–S_3 and S_5–S_7, are displayed in Fig. 3. The calibrated longitudinal dispersivity (α_L) and transverse dispersivity (α_T) were 7.0 cm and 0.5 cm, respectively, which are far lower than their respective initial values (45 cm and 4.5 cm). The difference between chloride and nitrate concentrations was used to calibrate the denitrification rate. *RMSE*s for the calibrated model are about 0.14 mg L^{-1} (n = 69, r^2 = 0.97, Fig. 3a) for chloride and 0.16 mg L^{-1} (n = 70, r^2 = 0.96, Fig. 3c) for nitrate. Corresponding observed concentrations (under bare-slope conditions) during the wet season were then used to validate the solute transport and reaction parameters. *RMSE*s for the validation run are 0.15 mg L^{-1} (n = 72, r^2 = 0.94, Fig. 3b) for chloride and 0.18 mg L^{-1} (n = 66, r^2 = 0.93, Fig. 3d) for nitrate. Simulated chloride and nitrate concentrations matched the observed data very well. The overall good description of observed groundwater tables and fluxes, and chloride and nitrate concentrations, implies that the calibrated parameters (Table 2) used in Hydrus-2D are reasonable.

Fig. 3e and f additionally show a comparison of experimental and simulated (with calibrated parameters) results during the wet season when the shoreline is covered with either lime or concrete, respectively. This comparison should validate the adequacy of applied boundary conditions at the downstream boundary, representing either an impermeable or partially permeable shoreline cover. The observed and simulated nitrate concentrations agreed well with a *RMSE* of 0.22 mg L^{-1} (n = 68, r^2 = 0.94; Fig. 3e) for a lime cover and a *RMSE* of 0.21 mg L^{-1} (n = 70, r^2 = 0.93; Fig. 3f) for a concrete cover. Consequently, the downstream boundary conditions for water flow (a seepage face above LWLs and a constant pressure head below LWLs) and solute transport are feasible.

Overall, Fig. 3 shows that chloride and nitrate had similar distributions (although at a different level due to nitrification, Fig. 3a and c) at all observation points. However, significant changes exist between the dry and wet seasons (Fig. 3a and b), which indicates that the LWL affected the solute transport into lake water. Additionally, as show in Fig. 3d–f (for the wet season), significant differences can be found in nitrate concentrations at S_1 and S_2 between bare-, lime-, and concrete-cover conditions. This implies that SRMs on the lakeshore slope affected the nitrate transport into the lakeshore zone.

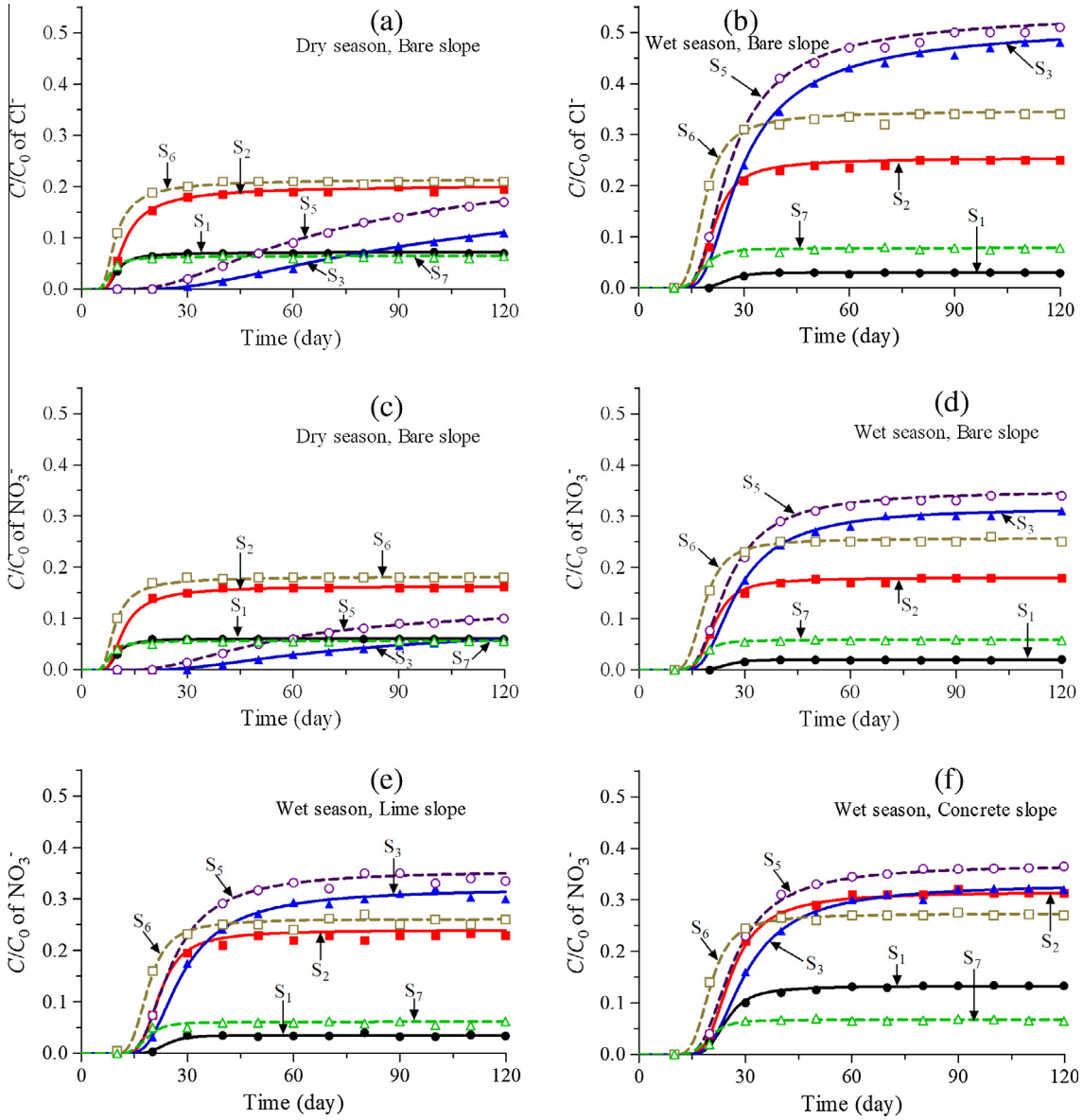

Fig. 3. Selected simulated and observed concentrations of chloride (Cl^-, a–b) and nitrate (NO_3^-, c–f) near the lakeshore slope under bare (for dry and wet seasons), lime (wet season), and concrete (wet season) slope cover (lines: simulated by Hydrus-2D; symbols: observed during the soil tank experiments). Results (for the dry season and the bare slope) displayed in (a) and (c) were used for model calibration and those (for the wet season and the bare slope) displayed in (b) and (d) for model validation. Results in (e) and (f) were used to test the validity of the downstream boundary condition. C_0: the input solute concentration from the fishpond/paddy field.

Table 2
Optimized values of the residual water content, θ_r, the saturated water content, θ_s, van Genuchten's shape parameters, α, and n, the saturated hydraulic conductivity, K_s, the longitudinal dispersivity, α_L, the transverse dispersivity, α_T, and the denitrification rate, K_{dn}.

Material	Soil type	θ_r ($cm^3\ cm^{-3}$)	θ_s ($cm^3\ cm^{-3}$)	α (cm^{-1})	n	K_s ($cm\ day^{-1}$)	α_L (cm)	α_T (cm)	K_{dn} (day^{-1})
Lakeshore	Loamy sand	0.055	0.40	0.121	2.16	338.9	7.0	0.5	0.015
Lime	Loamy sand	0.090	0.35	0.061	1.45	30.2	7.0	0.5	0.015

3.2. Groundwater table gradients in the lakeshore zone

Both GWT and LWL control the hydrology of the lakeshore zone as well as its transmissivity. In particular, compared to a relatively stable GWT, the LWL is subjected to frequent fluctuations in response to rainfall and wind waves on the lake shoreline. Additionally, the LWL can, in general, gradually rise or fall during an entire hydrological year. However, SRMs on the slope alter the hydrological cycle in the lakeshore zone and the associated transport and transformation of solutes. Fig. 2 shows the position of the GWT corresponding to three different LWLs. GWT gradients increased with the decline of the LWL, providing that the GWT remained stable off the lakeshore zone. During the dry season, the GWT under bare-slope conditions connected smoothly with lake water, with an average gradient of about 2.2%. On the other hand, under lime- or concrete-slope conditions, the GWT gradients in the lakeshore zone were smaller overall, but precipitously dropped near the slope face. Lee (2000) has also observed a rapid, steep water table mounding in

the near-shore region of Lake Barco (in Florida, USA). During the normal and wet seasons, the gradients near the slope face were affected by SRMs. The gradients were smaller when the surface was covered with concrete as compared to the lime cover. Thus, it can be seen that SRMs affected the GWT gradients once the lake water submerged a part of the SRM. Overall, based on simulated results, there was a relatively small increase in the groundwater table near the slope face when the shoreline was covered with concrete rather than with lime. Beneath the fishpond (100 cm from an upstream boundary), a barely visible mound of GWT occurred due to the continuous vertical flux from the fishpond.

3.3. Water flux distributions on the slope-face

The distribution of water fluxes (per a unit width of the tank and per a unit length of the slope face) on the slope face was significantly different for different SRMs during three seasons (Fig. 4 left). Overall, the maximum fluxes declined when the LWL increased (from levels for the dry season to the wet season). For the concrete-cover conditions (Fig. 4a–c), the distribution of water fluxes were similar for all three seasons (i.e., wet, normal, and dry) and occurred within the same spatial extent (OB, Fig. 1c). For the bare- and lime-cover conditions, the spatial extent of water fluxes on the slope increased with an increase in the LWL. The major water fluxes occurred in a narrow range of the slope face near the water level in the lake (LWL). During the dry season, the maximum fluxes for the bare-, lime-, and concrete-slope conditions were 175.1, 102.3, and 286.2 cm day^{-1}, respectively, and they were all located near point B (the bottom end of SRM, Fig. 4). When lime was used as a cover material, two flux peaks existed during both normal and wet seasons, reflecting the location of two materials (soil and lime) on the slope. One peak was located at point B (the bottom end of the lime cover), and another at point C or D (the corresponding intersect points of the LWL with the slope face during the normal and wet seasons, respectively, Fig. 1b and c). Overall, water fluxes near the slope bottom (point O) were very low, implying that only little water exchange occurred between groundwater and lake water at this location.

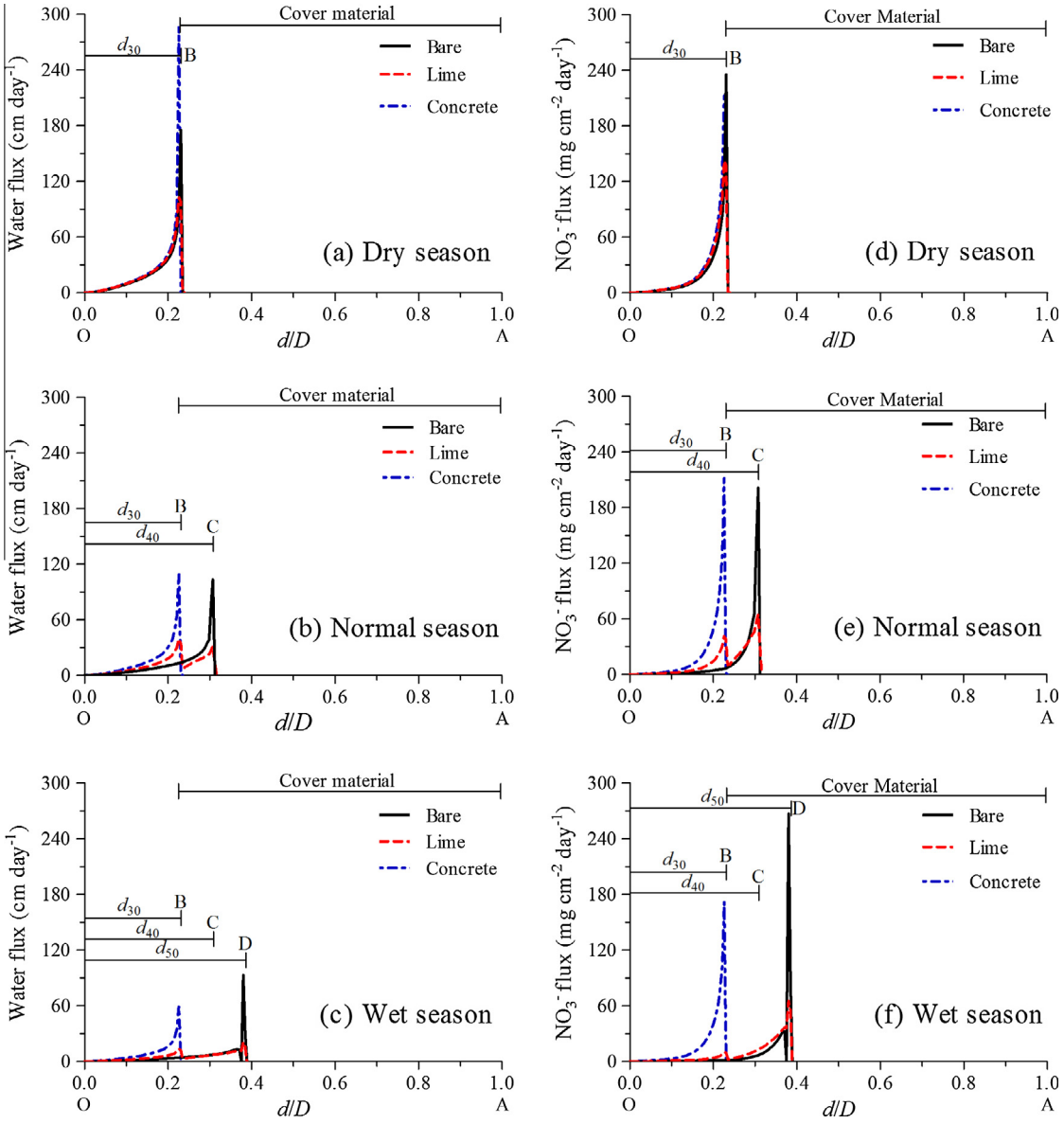

Fig. 4. Distributions of water (left) and nitrate (right) fluxes along the slope under bare-, lime-, and concrete-slope conditions at 120 day during the dry (a, d), normal (b, e), and wet (c, f) seasons. See Fig. 1c for the definition of letters A, B, C, D, and O.

3.4. Solute concentration and flux distributions on the slope-face

While nitrate flux distributions (per a unit width of the tank and a unit length of the slope face) along the lakeshore slope are displayed in Fig. 4 (right), the solute concentration distributions (for both chloride and nitrate) along the lakeshore slope are shown in Fig. 5. In general, solute fluxes closely resemble water fluxes (Fig. 4 left). Also, chloride and nitrate concentration distributions along the slope face are very similar (Fig. 5). While both chloride and nitrate are not retarded, nitrate concentrations are reduced due to denitrification. Positions (d/D) of peak values of chloride concentrations were slightly higher than those of nitrate during the three seasons under the bare-, lime-, and concrete-slope conditions. Differences in solute concentrations in the three seasons mainly resulted from different ratios of the water flux from the fishpond (which was constant) to the groundwater flux (which decreased with an increase in the LWL). As the water level in the lake increased, the solute concentrations on the slope also gradually increased (due to the higher ratio of the fishpond flux to the groundwater flux). On the other hand, as the overall thickness of the groundwater increased, water and solute fluxes decreased, resulting in more vertical solute dispersion (Figs. 5 and 6). A common phenomenon was that all peak values were located in the SRM zone (namely above point B, Fig. 1c and Fig. 4 right), even during the dry season (when the LWL was at point B).

When SRMs were partly submerged in lake water during the normal and wet seasons, the solute distributions on the slope face were affected by the SRMs (Fig. 5b and c). Although solute concentrations along the slope were more broadly distributed than water fluxes, solute fluxes closely reflected water fluxes, being concentrated in a narrow portion of the slope (Fig. 4 right). Major nitrate transport occurred through a narrow zone at the upper slope-face. Except for the concrete-slope (assumed no-flow) conditions, a small portion of solute transport occurred through the seepage face above the LWL (Fig. 6).

Fig. 5 shows that solute flux distributions on the slope face are different from water flux distributions. Water fluxes displayed two peaks during the normal and wet seasons when two surface

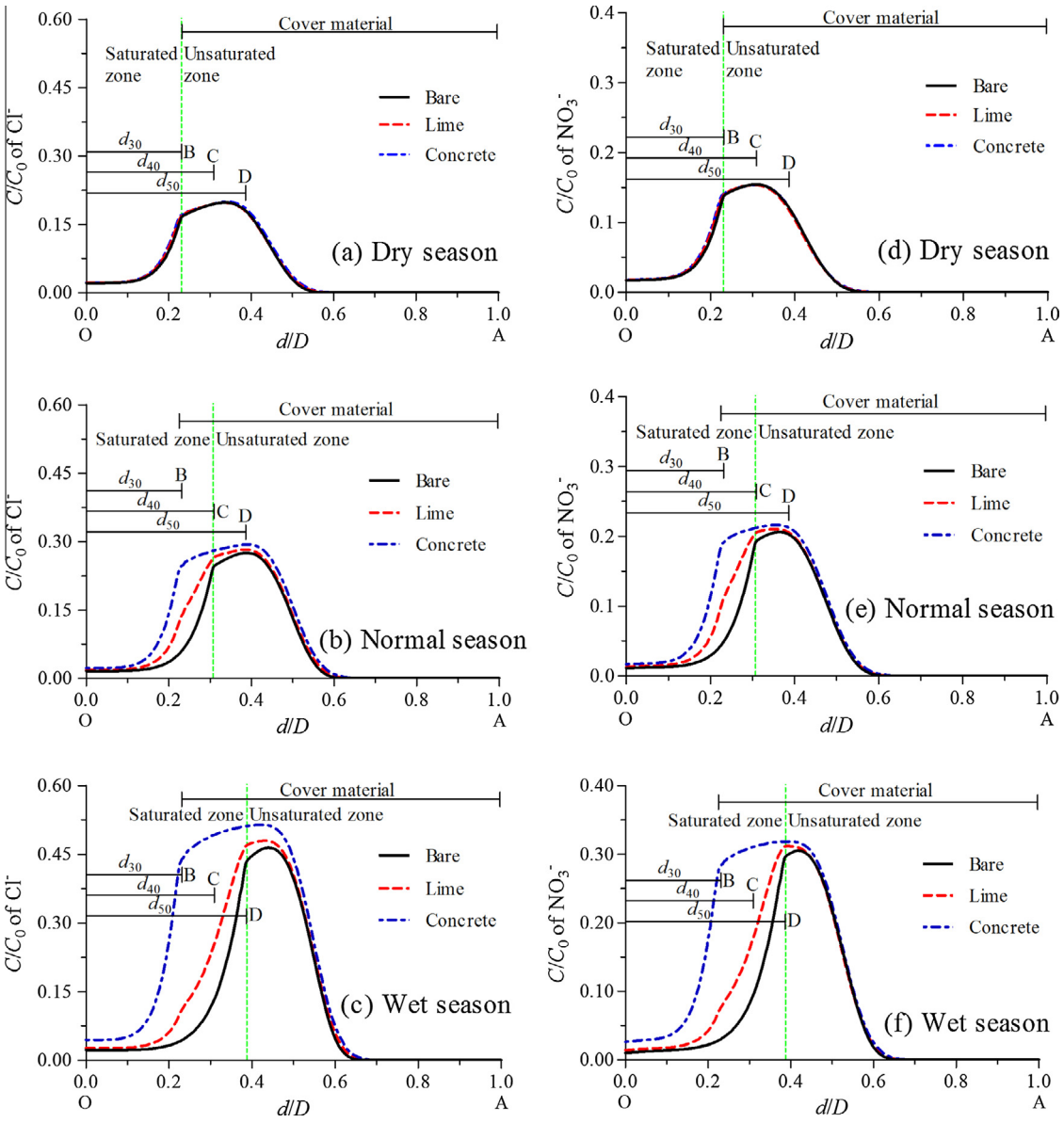

Fig. 5. Distributions of chloride (left) and nitrate (right) concentrations on the slope under bare-, lime-, and concrete-slope conditions at 120 day during the dry (a, d), normal (b, e), and wet (c, f) seasons. See Fig. 1c for the definition of letters A, B, C, D, and O. The vertical green dashed lines indicate the extent of saturated and unsaturated zones. C_0: the input solute concentration from the fishpond/paddy field.

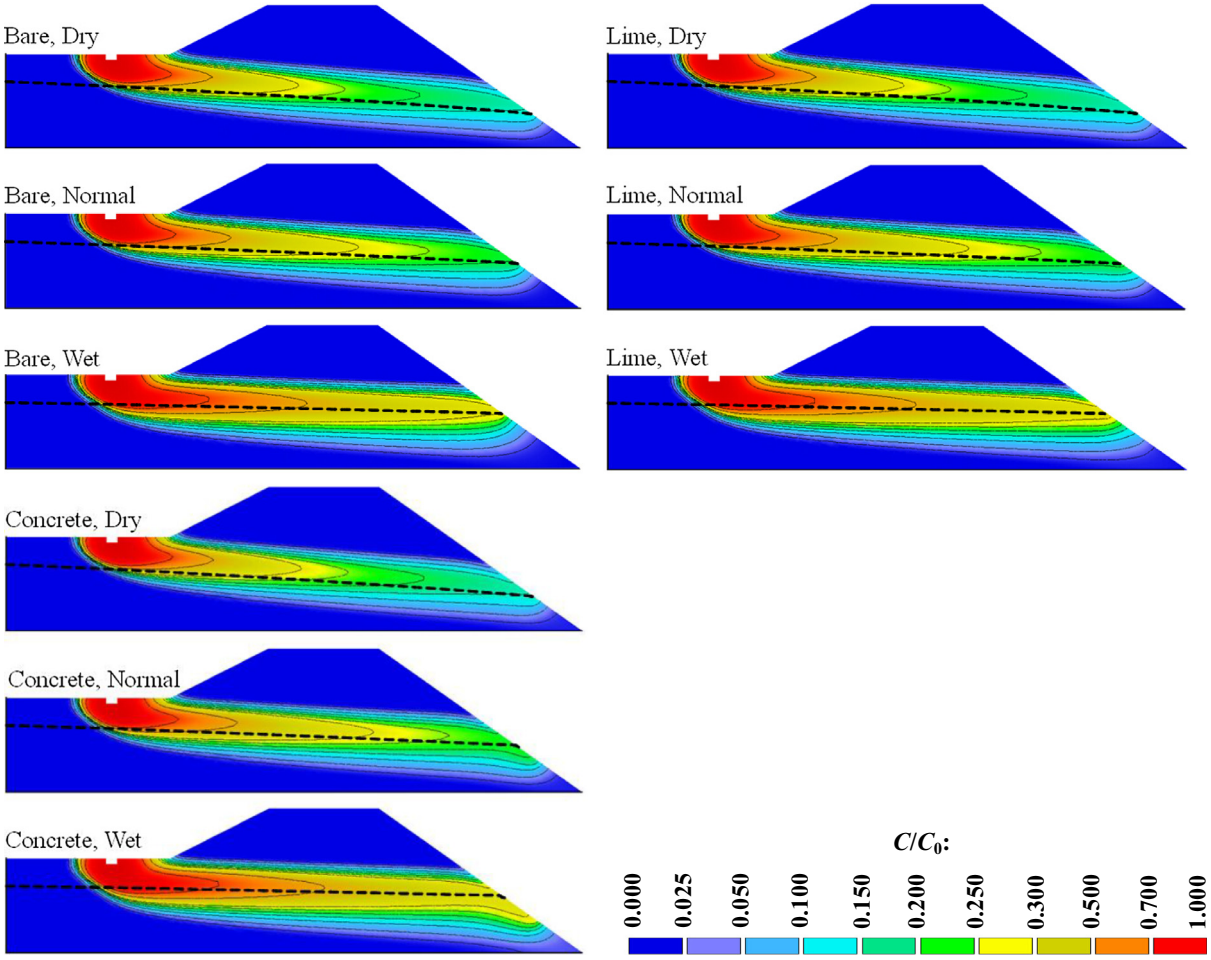

Fig. 6. Relative concentration (C/C_0) profiles of nitrate at 120 day under bare-, lime-, and concrete-slope conditions during the dry, normal, and wet seasons. The dashed line indicates the groundwater table. C_0: the input nitrate concentration from the fishpond/paddy field.

materials (i.e., lime and soil, or concrete and soil) were used on the slope face. Fig. 6 also shows that in the lakeshore zone, peaks of nitrate concentrations during the dry and normal seasons occurred above those of the GWT, while during the wet season they were near the GWT. As the LWLs increased, nitrate concentration plumes became more extended in both horizontal and vertical directions. Higher LWLs thus shortened the water and nitrate transport pathways. Additionally, as the hydraulic conductivity of the cover material decreased (for example from bare, to lime, and to concrete), more nitrate was transported through the slope face at the bottom of the slope (at point O). Particularly for the concrete cover, the SRM significantly altered both the water and nitrate flow paths (Fig. 6).

3.5. Water and solute transport through the seepage face

Due to the presence of a seepage face on the slope above the LWL, water and solutes flowed into the lake through both the seepage face and the submerged zone (Fig. 6). The water flux (per a unit width of the tank) decreased with the decline in the hydraulic permeability of SRMs from bare conditions, to lime, and to concrete (Fig. 7a). Differences in the total flux became more significant during the normal and wet seasons when a part of the SRMs were submerged. During the dry season, the fraction of the total flux due to the flux through the seepage face declined from 8.5% for a bare soil, to 2.2% for a lime cover, and to zero for a concrete cover. During the normal and wet seasons, these fractions dropped from 9.1% to 4.3%, and to zero, and from 6.7% to 2.9%, and to zero, respectively.

A fraction of solutes transported through the unsaturated zone and the seepage face was in general larger than a corresponding fraction of water. For the conservative solute chloride, the quantity traveling through the submerged zone on the slope face was almost the same for all conditions (Fig. 7b). On the other hand, the quantities of chloride traveling through the seepage face were significantly different, and decreased with the decline in the hydraulic conductivity of SRMs. The difference in the chloride flux (per a unit width of the tank) between different scenarios mostly resulted from the solute flux through the seepage face. On the other hand, the chloride fluxes through the seepage face declined with the increase of the LWL for all SRM conditions.

The nitrate fluxes (per a unit width of the tank) through both the seepage face and the submerged zone are markedly lower than the chloride fluxes due to denitrification. During the dry season, the nitrate fluxes through the submerged zone were almost the same for different SRM conditions (Fig. 7c), while through the seepage face they decreased from 242.5 mg cm^{-1} day^{-1} for bare soil, to 138.0 mg cm^{-1} day^{-1} for a lime cover, and to zero for a concrete cover. However, during the normal and wet seasons, the nitrate fluxes through both the seepage face and the submerged zone decreased with a decline in the hydraulic conductivity of SRMs. A decline in the total solute fluxes through the seepage face was much more significant than through the submerged zone. During the dry, normal, and wet seasons, the ratios of the solute flux

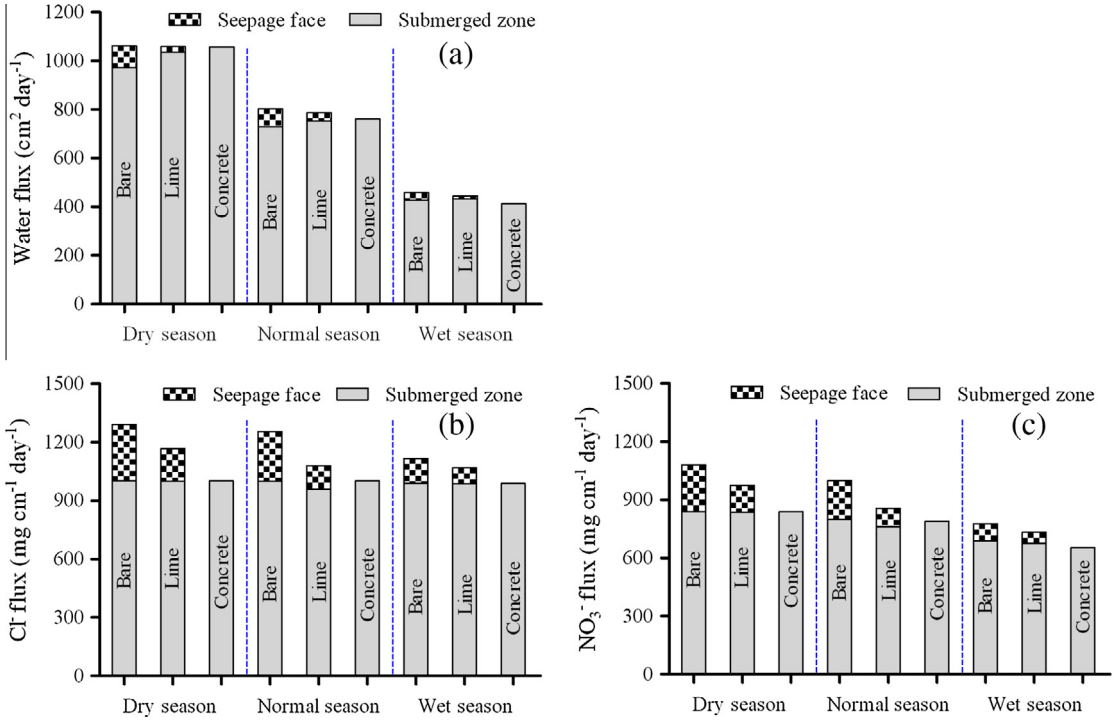

Fig. 7. Fluxes of water (a), chloride (b), and nitrate (c) through the seepage face and the submerged zone of the slope face under bare-, lime-, and concrete-covered conditions at 120 day during the dry, normal, and wet seasons.

through seepage face to the total solute flux decreased from 22.4% for bare soil, to 14.2% for a lime cover, and to zero for a concrete cover, from 20.2% (bare), to 11.1% (lime), to zero (concrete), and from 11.4% (bare), to 7.6% (lime), to zero (concrete), respectively.

4. Discussion

4.1. Flux distributions on the slope-face

Previous studies have reported that the flux distribution along a slope-face follows an exponential function, increasing with the distance from the lake bottom (McBride and Pfannkuch, 1975; Winter, 1978; Shaw et al., 1990). Namely, the flux gradually increases with d/D and rapidly ascends near the LWL on the slope face. Shaw et al. (1990) found, based on field observations using seepage meters in Narrow Lake (Alberta), that the average seepage flux decreased with the distance from the shore. Genereux and Bandopadhyay (2001) reported, using MODFLOW simulations, that seepage rates on a lakebed could be fitted well with an exponential function. Li and Wang (2007) also reported that the seepage flux along a lakeshore could be well fitted with an exponential function, and that the largest fluxes occurred within a narrow portion of the slope near the LWL. Our simulations (Fig. 4) confirm these results when the hydraulic conductivity of the slope face is uniform, such as under bare-slope conditions. For three LWLs, half of all water enters the lake within 0.18D, 0.24D, and 0.31D from point O under bare-slope conditions, and within 0.23D, 0.31D, and 0.38D under lime-slope conditions, respectively. Very similar results were previously reported in the literature. For example, Lee (2000) reported for hypothetical steady-state conditions that all predicted groundwater inflow into Lake Barco occurred within 5 m off the shore in water less than 0.4 m deep, and the majority of inflow occurred within 3 m off the shore in water less than 0.3 m deep. Wilson and Gardner (2006) also found that, at all stages of the tide, the largest velocities of groundwater flow developed just below the intersection of the tide at the river bank, and most flow occurred within 15 m of the river.

However, some field studies have shown non-exponential relationships of the seepage flux on the slope face (Cherkauer and Nader, 1989; Shaw and Prepas, 1990; Schneider et al., 2005). This is because hydraulic properties (such as the hydraulic conductivity) were unevenly distributed along the slope face in most field studies. Kishel and Gerla (2002) found a high degree of seepage heterogeneity across a 170-m^2 area near the lakeshore of the Shingobee Lake (USA). Likewise, Guyonnet (1991) showed how small-scale sediment variations in relatively thin, either high- or low-permeability layers can have a significant effect on the seepage distribution. Genereux and Bandopadhyay (2001) reported that low-permeability lakebed sediments could have a major effect on the spatial distribution of the lake-bed seepage in both inflow or flow-through lakes, even when the sediments are of a constant thickness over the entire lake bed. The lower the permeability of lake-bed sediments, the more even the distribution of seepage fluxes. In a small area examined, the discharge flux irregularly decreased with the distance into the lake, indicating that sediment heterogeneity plays an important role in the distribution of groundwater discharge (Kishel and Gerla, 2002). In addition to these factors, the regional hydrogeology significantly affects the seepage distribution on the slope face. Our simulated results also show that when different types of materials cover the slope face, the flux distribution does not follow the exponential distribution (Fig. 4). These conflicting results suggest that underlying processes controlling the lakeshore seepage need additional clarification (Schneider et al., 2005).

The well-fitted exponential distributions were usually derived for hypothetical or theoretical conditions using mostly model simulations, rather than collected experimental data. Additionally, the vertical hydraulic conductivity significantly affected the seepage flux distributions. Genereux and Bandopadhyay (2001) found that seepage rates along the lake bed simulated using the 2D MODFLOW model were significantly different from those simulated using the 3D model.

Furthermore, we can see that the exchange of water and solutes at the slope bottom (near point O) was significantly smaller compared to those at points B, C, and D during three seasons (Fig. 6). This implies that solutes accumulate near point O. Many studies (i.e. Fischer et al., 2005; Boulton et al., 2010; Stelzer et al., 2011) reported that nutrients or pollutants are prone to accumulate at the bottom of the hyporheic zone.

4.2. Seepage face

A portion of water flowing through a seepage face is an important characteristic of the exchange between ground water and surface water. Many simulated and observed results have reported the existence of a seepage face and its effects on water flow and solute transport (Vachaud et al., 1973; Simpson et al., 2003; Rushton, 2006; Chenaf and Chapuis, 2007). For example, in a sand box experiment involving radial flow and transport, Simpson et al. (2003) found that the flow velocity through the seepage face was about 30% higher than at the base of the aquifer, while the solute transport patterns were strongly influenced by the flow characteristics of the system. Yakirevich et al. (2010) also reported that a seepage face might be responsible for causing the early arrival of solutes and the overall shape of the BTCs. Yuan et al. (2011) reported that if the solute originates from the near shore surface land, such as wetlands, the solute flux from the seepage face provides an important source of solute for surface water.

Our simulated results show that when the source of surface pollution is on the land surface near the lake, both water and pollutants flow into the lake partly through the seepage face (Figs. 6 and 7). Moreover, the ratios of water and solute fluxes through the seepage face to the total fluxes through the entire slope face fluctuate with the LWL. They accounted for about 6.7–9.1% of the total discharge under bare-slope conditions, while they were only about 2.2–4.3% under lime-slope conditions. The seepage face length on the slope face is easily influenced by the surface water level, which is further affected by wind waves and precipitation. However, we could not confirm that the seepage face has an accelerating effect on the solute transport due to different flow paths to the slope face. The distribution of hydraulic conductivity on the slope face also affects the seepage face length.

Additionally, the seepage face is also a connecting interface between groundwater and atmosphere. Groundwater flows through the soil towards an open boundary where the environmental factors, which may affect various reaction rates such as nitrification and denitrification, are very different. Burgin and Groffman (2012) reported that soil O_2 was consistently lower in the area closest to the stream and increased further from the stream. In this case, the nitrification rate increases and the denitrification rate decreases rapidly near the seepage face (Burgin and Groffman, 2012).

5. Conclusions

Lakeshore is an important transition zone connecting lake water and surrounding groundwater. The hydrological connectivity significantly affects the exchange of water and solutes between surface waters and groundwater and the flux distribution of water and solutes on the slope face. Slope revetment materials artificially change the local hydrological connectivity by altering the hydraulic conductivity of the slope face and consequently change the hydrological dynamics and nutrient discharge into lake water.

Based on the soil tank experiments and Hydrus-2D simulations, the distributions of water and solute fluxes and solute concentrations on the shoreline face depend largely on the distribution of the soil hydraulic conductivity of the slope face. Uneven distribution of the hydraulic conductivity results in a non-exponential distribution of water and solute fluxes. Most water and solute discharge into the lake within a narrow zone near the intersection point of the lake water level and the slope face. Relatively low-conductivity slope revetment materials change the seepage flow path, increase the seepage face length, and increase the ratio of water and solutes transported through the unsaturated zone. These changes may affect denitrification processes in the near-shore region, by changing local water contents in the lakeshore zone. Relatively low exchange of water and solutes at the lakeshore bottom may lead to the accumulation of pollutants at the bottom of the hyporheic zone. The Hydrus-2D model proved to be a useful tool for analyzing the hydrodynamics and solute transport in a lakeshore zone and for providing better understanding of associated factors and processes.

Acknowledgements

This work was supported by the National Natural Science Foundation of China (No: 51079048), the Ministry of Education Key Laboratory of Integrated Regulation and Resource Development on Shallow Lakes (No: 2008KJ003), the Water Conservancy Science and Technology Project of Jiangsu Province (No: 2013071), and the China Scholarship Council.

References

Bouazza, A., Freund, M., Nahlawi, H., 2006. Water retention of nonwoven polyester geotextiles. Polym. Testing 25 (8), 1038–1043.
Boulton, A.J., Datry, T., Kasahara, T., Mutz, M., Stanford, J.A., 2010. Ecology and management of the hyporheic zone: stream-groundwater interactions of running waters and their floodplains. J. North Am. Benthol. Soc. 29 (1), 26–40.
Burgin, A.J., Groffman, P.M., 2012. Soil O_2 controls denitrification rates and N_2O yield in a riparian wetland. J. Geophys. Res. 117, G01010. http://dx.doi.org/10.1029/2011JG001799.
Cey, E.E., Rudolph, D.L., Parkin, G.W., Aravena, R., 1998. Quantifying groundwater discharge to a small perennial stream in southern Ontario, Canada. J. Hydrol. 210, 21–37.
Chenaf, D., Chapuis, R.P., 2007. Seepage face height, water table position, and well efficiency at steady state. Ground Water 45 (2), 168–177.
Cherkauer, D.S., Nader, D.C., 1989. Distribution of groundwater seepage to large surface-water bodies: the effect of hydraulic heterogeneities. J. Hydrol. 109 (1–2), 151–165.
Fischer, H., Kloep, F., Wilzcek, S., Pusch, M.T., 2005. A river's liver – microbial processes within the hyporheic zone of a large lowland river. Biogeochemistry 76 (2), 349–371.
Gelhar, L.W., Mantoglou, A., Welty, C., Rehfeldt, K.R., 1985. A review of field-scale physical solute transport processes in saturated and unsaturated porous media. EPRI Rep. EA-4190, Elec. Power Res. Inst., Palo Alto, Calif., August.
Genereux, D., Bandopadhyay, I., 2001. Numerical investigation of lake bed seepage patterns: effects of porous medium and lake properties. J. Hydrol. 241, 286–303.
Guyonnet, D.A., 1991. Numerical modeling of effects of small-scale sedimentary variations on groundwater discharge into lakes. Limnol. Oceanogr. 36 (4), 787–796.
Howarth, R., Chan, F., Conley, D.J., Garnier, J., Doney, S.C., Marino, R., Billen, G., 2011. Coupled biogeochemical cycles: eutrophication and hypoxia in temperate estuaries and coastal marine ecosystems. Front. Ecol. Environ. 9 (1), 18–26.
Hu, X., Xu, Q., Jiang, L., Dong, S., Jin, D., 2011. A preliminary study on demarcation limits of lake buffer zones: a case study of Lake Taihu. J. Lake Sci. 23 (5), 719–724.
Kidmose, J., Engesgaard, P., Nilsson, B., Laier, T., Looms, M.C., 2011. Spatial distribution of seepage at a flow-through lake: Lake Hampen, Western Denmark. Vadose Zone J. 10, 110–124.
Kishel, H.F., Gerla, P.J., 2002. Characteristics of preferential flow and groundwater discharge to Shingobee Lake, Minnesota, USA. Hydrol. Proc. 16 (10), 1921–1934.
Lamy, E., Lassabatere, L., Bechet, B., Andrieu, H., 2013. Effect of a nonwoven geotextile on solute and colloid transport in porous media under both saturated and unsaturated conditions. Geotext. Geomembr. 36, 55–65.
Lassabatere, L., Winiarski, T., Galvez Cloutier, R., 2004. Retention of three heavy metals (Zn, Pb, and Cd) in a calcareous soil controlled by the modification of flow with geotextiles. Environ. Sci. Technol. 38 (15), 4215–4221.
Lee, T.M., 2000. Effects of nearshore recharge on groundwater interactions with a lake in mantled karst terrain. Water Resour. Res. 36 (8), 2167–2182.
Li, Y., Wang, C., 2007. Theoretical estimation of groundwater discharge and associated nutrient loading to a lake with gentle slope bottom. J. Hydrodyn. Ser. B 19 (1), 30–35.
Li, Y., Wang, C., Yang, L.Z., Li, Y.P., 2007. Influence of seepage face obliquity on discharge of groundwater and its pollutant into lake from a typical unconfined aquifer. J. Hydrodyn. Ser. B 19 (6), 756–761.
McBride, M.S., Pfannkuch, H.O., 1975. Distribution of seepage within lake beds. J. Res. United States Geol. Surv. 3, 505–512.

Mohamed, T.A., 2006. Evaluation of environmental and hydraulic performance of bio-composite revetment blocks. Am. J. Environ. Sci. 2 (4), 129–134.
Nahlawi, H., Bouazza, A., Kodikara, J., 2007. Characterisation of geotextiles water retention using a modified capillary pressure cell. Geotext. Geomembr. 25 (3), 186–193.
Ostendorp, W., 2004. New approaches to integrated quality assessment of lakeshores. Limnologica 34, 160–166.
Phogat, V., Mahadevan, M., Skewes, M., Cox, J.W., 2012. Modelling soil water and salt dynamics under pulsed and continuous surface drip irrigation of almond and implications of system design. Irrig. Sci. 30 (4), 315–333.
Rushton, K.R., 2006. Significance of a seepage face on flows to wells in unconfined aquifers. Quart. J. Eng. Geol. Hydrogeol. 39 (4), 323–331.
Schneider, R.L., Negley, T.L., Wafer, C., 2005. Factors influencing groundwater seepage in a large, mesotrophic lake in New York. J. Hydrol. 310 (1–4), 1–16.
Shaw, B.R., Radler, B.T., Haack, J., 2011. Exploring the utility of the stages of change model to promote natural shorelines. Lake Reserv. Manage. 27, 310–320.
Shaw, R.D., Prepas, E.E., 1990. Groundwater-lake interactions: II. Nearshore seepage patterns and the contribution of ground water to lakes in central Alberta. J. Hydrol. 119, 121–136.
Shaw, R.D., Shaw, J.F.H., Fricker, H., Prepas, E.E., 1990. An integrated approach to quantify groundwater transport of phosphorus to Narrow Lake, Alberta. Limnol Oceanogr. 35 (4), 870–886.
Simpson, J.M., Clement, T.P., Gallop, T.A., 2003. Laboratory and numerical investigation of flow and transport near a seepage-face boundary. Ground Water 41 (5), 690–700.
Šimůnek, J., van Genuchten, M.T., Šejna, M., 2008. Development and applications of the HYDRUS and STANMOD software packages, and related codes. Vadose Zone J. 7 (2), 587–600.
Šimůnek, J., van Genuchten, M.T., Šejna, M., 2012. The HYDRUS Software Package for Simulating the Two- and Three-Dimensional Movement of Water, Heat, and Multiple Solutes in Variably-Saturated Porous Media. PC-Progress, Prague.
Stelzer, R.S., Bartsch, L.A., Richardson, W.B., Strauss, E.A., 2011. The dark side of the hyporheic zone: depth profiles of nitrogen and its processing in stream sediments. Freshw. Biol. 56, 2021–2033.
Vachaud, G., Vauclin, M., Khanji, D., Wakil, M., 1973. Effects of air pressure on water flow in an unsaturated stratified vertical column of sand. Water Resour. Res. 9 (1), 160–173.
van Genuchten, M.T., 1980. A closed-form equation for predicting the hydraulic conductivity of unsaturated soils. Soil Sci. Soc. Am. J. 44 (5), 892–898.
Wang, X., Luo, J., 2006. A preliminary study of ecological embankment construction for urban river restoration. J. Fudan Univ. (Nat. Sci.) 45 (1), 120–126.
Wilson, A.M., Gardner, L.R., 2006. Tidally driven groundwater flow and solute exchange in a marsh: numerical simulations. Water Resour. Res. 42, W01405. http://dx.doi.org/10.1029/2005WR004302.
Winter, T.C., 1978. Numerical simulation of steady-state three dimensional groundwater flow near lakes. Water Resour. Res. 14 (2), 245–254.
Yakirevich, A., Gish, T.J., Šimůnek, J., van Genuchten, M.T., Pachepsky, Y.A., Nicholson, T.J., Cady, R.E., 2010. Potential impact of a seepage face on solute transport to a pumping well. Vadose Zone J. 9, 686–696.
Yang, H., Zhang, H., Zhao, Y., Feng, F., Yu, Z., 2005. An engineering method for restoration of the damaged riparian ecosystem using Phragmites australis. Chinese J. Ecol. 24 (2), 214–216.
Yao, S., Yue, H., 2012. Development trend of eco-revetment works in middle and lower reaches of Yangtze River. China Water Res. 6, 18–21 (In Chinese with English Abstract).
Yuan, L., Xin, P., Kong, J., Li, L., Lockington, D., 2011. A coupled model for simulating surface water and groundwater interactions in coastal wetlands. Hydrol. Process. 25, 3533–3546.
Zhu, W., Wang, Y., Lei, S., 2012. Effect of the control measures closing to nature on slope gradient of relative balance for river bank: a case study of the Taohua River in Changshou District, Chongqing City. Sci. Soil Water Conserv. 10 (3), 36–42 (In Chinese with English Abstract).